Biocontaminant

Original Research

Open Access

https://doi.org/10.48130/biocontam-0025-0004

Metabolic responses and biodegradation pathways of microalgal-bacterial granular sludge to estriol: structural remodeling, microbial shifts, and gene dynamics

Yuting Shi[1,2], Changqing Chen[1], Bingyi Ding[1], Yaorong Shu[3], Jie Feng[1], Anjie Li[4] and Bin Ji[1*]

Received: 4 September 2025

Revised: 24 September 2025

Accepted: 13 October 2025

Published online: 3 November 2025

Abstract

The persistence of endocrine-disrupting compounds such as estriol (E3) in wastewater presents a critical challenge for conventional treatment systems. This study investigates the metabolic responses and biodegradation pathways of microalgal-bacterial granular sludge (MBGS) under varying E3 concentrations (0, 0.1, 1, and 10 mg/L). The results indicate a concentration-dependent effect of E3 on MBGS performance. At 0.1 mg/L E3, COD removal was enhanced, correlating with an increased abundance of *Sphaerotilaceae* and their elevated contribution to the *fccA* gene. In contrast, higher concentrations (1 and 10 mg/L) severely disrupted the filamentous structure of *Cyanobacteria*, resulting in diminished removal efficiencies for COD, NH_4^+-N, and PO_4^{3-}-P. Metabolically, E3 was first oxidized to E1 and then converted into less toxic intermediate metabolites, achieving 97.9% and 85.7% removal at 0.1 mg/L during the day and night, respectively. Metagenomic analysis revealed that E3 altered the microbial community by suppressing the *Oculatellaceae, Leptolyngbyaceae,* and *Comamonadaceae,* while enriching the *Sphingomonadaceae, Rhodanobacteraceae,* and *Xanthomonadaceae*. These shifts led to disrupted microbial interactions and reduced abundance of key functional genes, including *mqo*, *GLU*, *ppk1*, and *atpA*. Importantly, E3 biodegradation was primarily facilitated by *Sphingomonadaceae* and *Rhodanobacteraceae* through their heightened contributions of core catabolic genes (*hshA*, *hsaA*, *hsaB*, *hsaC*, and *xylE*). In the meantime, *Xanthomonadaceae* contributed to energy maintenance via the *atpA* gene. These findings demonstrate the adaptive capacity of MBGS to estrogenic stress, offering insights into its potential application for sustainable wastewater treatment.

Keywords: Microalgal-bacterial symbiosis, Estriol, Endocrine-disrupting compound, Biological metabolism, Functional structure

Highlights

- MBGS effectively removed 0.1 mg/L estriol (E3) with > 97% efficiency during the day.
- 1 and 10 mg/L E3 significantly disrupt the cell structure of *Cyanobacteria*.
- E3-induced dynamic regulation of EPS is adaptive defense mechanism of MBGS.
- Structural damage to *Cyanobacteria* led to disrupted microbial interactions.
- *Sphingomonadaceae* and *Rhodanobacteraceae* drive E3 biodegradation via key catabolic genes.

* Correspondence: Bin Ji (binji@wust.edu.cn)

Full list of author information is available at the end of the article.

Graphical abstract

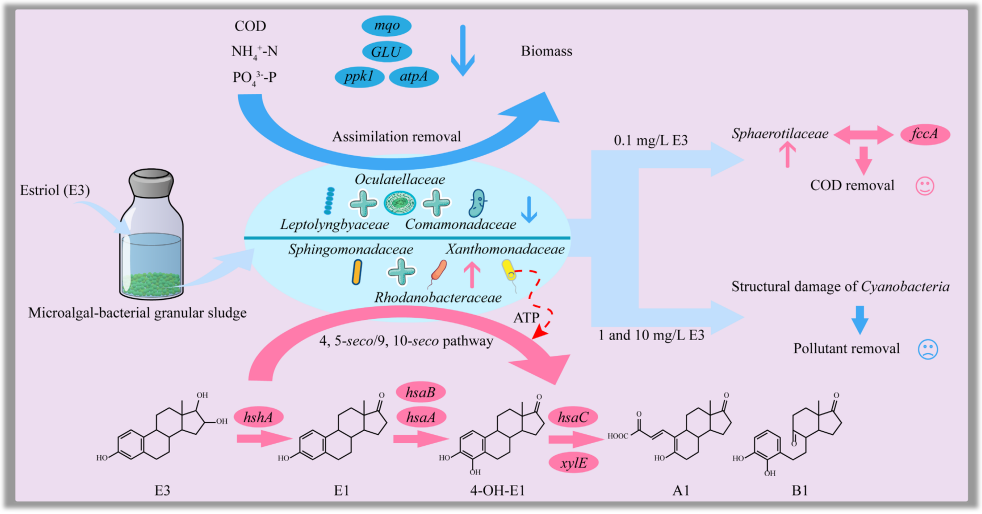

Introduction

In recent years, increasing attention has been directed toward the widespread occurrence of endocrine-disrupting compounds (EDCs) in aquatic environments, owing to their persistence, bioactivity, and potential risks to ecological and human health[1,2]. Among these, estriol (E3), a naturally occurring estrogen, has been frequently detected in domestic sewage, hospital effluents, and discharges from municipal wastewater treatment plants[3–5]. Although environmental concentrations of E3 are typically in the range of ng/L to μg/L[6,7], its high estrogenic potency enables it to exert biological effects at sub-nanogram levels, thereby raising concerns even at trace exposure concentrations[8,9]. Moreover, it can range from μg/L to mg/L in hospital wastewaters, pharmaceutical manufacturing effluents, and pig farm wastewaters[10,11], posing a considerable challenge to conventional treatment systems.

Conventional wastewater treatment technologies, particularly activated sludge systems, often exhibit limited efficiency in removing estrogens[12,13], primarily due to their low biodegradability and resistance to microbial degradation[14]. Meanwhile, advanced physicochemical methods, such as ozonation, advanced oxidation processes, and adsorption, although capable of improving removal efficiencies, often involve high capital and operational costs, complex operations, and a risk of forming toxic transformation byproducts[15–17]. Although pure cultures (e.g., *Novosphingobium* sp.) can effectively degrade E3, their sensitivity to environmental fluctuations and lack of functional redundancy stand in sharp contrast to the robustness of complex microbial communities in the microalgal-bacterial granular sludge (MBGS) system[18].

MBGS has emerged as a promising sustainable solution for wastewater treatment, integrating the complementary roles of phototrophic microalgae and heterotrophic bacteria within a self-aggregated granular structure[19,20]. This system enhances the removal of organic matter and nutrients, promoting the biodegradation of recalcitrant micropollutants through diverse microbial consortia and internal oxygen cycling[21,22]. Notably, the dominance of *Proteobacteria* within MBGS[20], a phylum with known E3-degrading capabilities[18,23], suggests an inherent potential for E3 removal. Furthermore, the synergistic relationships between microalgae and bacteria can improve the adsorption, transformation, and mineralization of refractory compounds[21,24]. The structural integrity provided by *Cyanobacteria* is essential for granule stability and system resilience[25,26], and their sensitivity to high E3 stress is a critical determinant of the system's overall stability. However, their possible susceptibility to high E3 stress remains a key factor influencing overall system performance. Given its documented resilience to environmental perturbations and shock load[27,28], the MBGS system represents a compelling candidate for treating wastewaters containing high or fluctuating levels of E3. A systematic understanding of its metabolic responses and biodegradation pathways under sustained E3 exposure however, remains insufficient.

This study aims to investigate the metabolic responses and biodegradation pathways of the MBGS system when exposed to varying concentrations of E3 (0, 0.1, 1, and 10 mg/L). By integrating analysis of granule morphological characteristics, pollutant removal efficiency, and microbial community succession, this research aims to elucidate the adaptive responses of the MBGS system to varying E3 concentrations. This approach enables a comprehensive assessment of the MBGS system robustness, microbial adaptability, and functional gene responses under estrogenic stress. Insights from this work will contribute to a deeper understanding of E3 biodegradation mechanisms in MBGS systems, and inform the development of resilient and efficient biotechnological solutions for the treatment of EDC-contaminated wastewater.

Materials and methods

Synthetic wastewater and E3

Synthetic wastewater was formulated to contain 400.0 mg/L chemical oxygen demand (COD) (as CH_3COONa), 25.0 mg/L ammonia nitrogen (NH_4^+-N) (as NH_4Cl), and 3.5 mg/L phosphorus (PO_4^{3-}-P) (as KH_2PO_4). The required dosages were 527.0, 95.5, and 15.4 mg/L of each compound, respectively, whereas the other compositions are shown in Supplementary Table S1. The influent dissolved oxygen (DO) concentration was maintained at around 3.2 mg/L, while the pH and water temperature were controlled at about 7.4 and 22.5 °C, respectively.

E3 was purchased from Shanghai Aladdin Biochemical Technology Co., Ltd. (Shanghai, China). A stock solution was prepared by dissolving E3 in ultrapure water with 0.5 h of magnetic stirring, followed by 1.0 h of ultrasonication (40 kHz) using an ultrasonic

cleaner[29]. Synthetic wastewaters containing 0, 0.1, 1, and 10 mg/L E3 were prepared daily for experiments.

Experimental setup

The MBGS, sourced from previous work[20], had the following initial physical properties: average size of 2.8 mm, 5-min sludge volume index (SVI_5) of 46.5 mL/g, zone settling velocity (ZSV) of 1.5 cm/s, and volatile suspended solids (VSS) concentration of 4.0 g/L in all reactors. Daily experiments were conducted using 12 glass vials (organized into four groups with triplicate samples each) with an effective working volume of 100 mL. Illumination was provided by four LED lamps (MBTL-T8-18, Hangzhou Mobet Biotechnology Co., Ltd., China) to achieve a uniform light intensity of 200 μmol/m^2/s. The hydraulic residence time (HRT) was maintained at 12 h under a 12 h/12 h light/dark cycle. Influent and effluent samples were collected daily at 9:00 and 21:00 to assess the removal efficiencies of conventional pollutants (COD, NH_4^+-N, PO_4^{3-}-P) and E3 over 12 h intervals. MBGS samples were taken from each group on days 1 and 21 for further analysis. Batch experiments were performed using 24 glass vials (eight groups of triplicates) with an effective working volume of 50 mL, and spiked with 10 mg/L of E3. The experiments were conducted separately under light (day phase), and dark (night phase) conditions. Water samples were taken at time intervals of 0, 0.5, 1, 1.5, 2, 3, 4, 8, and 12 h to determine the kinetics of pollutant and E3 removal by the MBGS.

To evaluate the contribution of adsorption to E3 removal, batch adsorption experiments were conducted using autoclave-inactivated MBGS. MBGS obtained from the control reactor was sterilized via autoclaving at 121 °C for 30 min. This treatment effectively eliminated microbial activity while retaining the structural integrity and adsorption capacity of the extracellular polymeric substances (EPS). The inactivated biomass was subsequently rinsed with sterile phosphate-buffered saline (PBS; 0.1 M, pH 7.0) to eliminate soluble compounds released during autoclaving. All glass vials were incubated in the dark to preclude photodegradation. Liquid samples were collected at predetermined time intervals (0, 0.5, 1, 1.5, 2, 3, 4, 8, and 12 h), and promptly filtered through 0.22-μm nylon membrane filters for subsequent analysis.

For pollutant analysis, water samples were filtered through a 0.45 μm membrane and stored in a refrigerator at 4 °C for subsequent measurements. For E3 analysis, water samples were acidified to a pH of 3 with HCl, and stored at 4 °C in amber glass vials to prevent photodegradation. All water samples were analyzed within 24 h. Biomass samples for DNA extraction and EPS analysis were flash-frozen in liquid nitrogen and stored at −80 °C until processing to preserve biomolecular integrity.

Analytical methods

Pollutant concentrations and granular characteristics were measured using standard analytical methods[30]. The theoretical COD contribution from E3 was calculated based on its stoichiometric oxidation equation ($C_{18}H_{24}O_3 + 20O_2 = 18CO_2 + 12H_2O$), and deducted from measured influent and effluent values. Therefore, all reported COD removal efficiencies reflect only the removal of the underlying synthetic wastewater substrate. MBGS morphology was visualized using an inverted fluorescence microscope (Olympus IX83, Tokyo, Japan) and a scanning electron microscope (Gemini 500, Zeiss, Germany). The surface functional groups of EPS were analyzed by a Fourier transform infrared spectrometer (FT-IR, IRTracer 100, Shimadzu, Japan). Specific methods for detecting granule size, EPS (including protein (PN) and polysaccharide (PS)) content, 3D-EEM fluorescence spectrum of EPS, chlorophyll (Chl) content, and glycogen content of MBGS are described in Supplementary Text S1. Instruments used to measure light intensity, DO concentration, pH, and temperature during the experiment are presented in Supplementary Text S2.

E3 concentration and metabolism analyses

For the quantification of E3 concentration, water samples were analyzed using high-performance liquid chromatography (HPLC, Foley LC5090, Zhejiang Fuli Analytical, China) coupled with a UV detector[31]. The chromatographic separation was performed using a reversed-phase C18 column (250 mm × 4.6 mm i.d., 5 μm particle size; Shimadzu, Kyoto, Japan) maintained at 25 °C. Isocratic elution was employed using a mobile phase of HPLC-grade acetonitrile and ultrapure water (65:35, v/v) at a flow rate of 1.0 mL/min. Detection was carried out at 250 nm with an injection volume of 10.0 μL. The autosampler needle was rinsed with chromatographic-grade methanol between injections. Quantification was conducted using an external standard method based on a calibration curve. The method demonstrated excellent linearity ($R^2 > 0.999$) across the concentration range of 0.05–20 mg/L.

For metabolite analysis of E3, an ultra-high-performance liquid chromatography (UHPLC, ExionLC™ 2.0, Shimadzu, Japan) with a high-resolution mass spectrometry system (HRMS, QTOF X500R, AB SCIEX, USA) was used to analyze the effluent samples of 10 mg/L E3 addition[18]. Chromatographic separation was performed on an ACQUITY UPLC BEH C18 column (100 mm × 2.1 mm i.d., 1.9 μm; Waters, Milford, MA, USA) maintained at 50 °C. The mobile phase consisted of: (A) an aqueous solution containing 0.1% (v/v) formic acid; and (B) acetonitrile, with a flow rate of 0.3 mL/min and an injection volume of 4 μL. Mass spectrometric detection was conducted using electrospray ionization (ESI) in both positive/negative modes with the following parameters: capillary voltage, 5 kV; curtain gas, 35 psi; desolvation temperature, 550 °C; nebulizer gas, 50 psi; auxiliary gas, 50 psi; and nitrogen as the collision gas. The scanning mode was information-dependent acquisition (IDA), with the mass range of 50~1,050 Da, and the voltage parameters included de-clustering voltage 80 V, MS1 fragmentation voltage 10 V and MS2 fragmentation voltage 35 V. In addition, E3 and its eventual degradation products were analyzed for toxicity prediction, including the bioconcentration factor and mutagenicity, using TEST 5.1.2.0 software[32].

Metagenomic sequencing analysis

Genomic DNA was extracted from MBGS samples using the FastPure Soil DNA Isolation Kit (MJYH, Shanghai, China) and assessed by 1% agarose gel electrophoresis. The DNA was sheared to approximately 350 bp fragments using a Covaris M220 instrument, followed by library construction (paired-end, bridge PCR) and Illumina sequencing[33]. Open reading frames (ORFs) were predicted from assembled contigs with Prodigal v2.6.3, and a non-redundant gene catalog was constructed using CD-HIT. Gene abundance was quantified by aligning high-quality reads to this catalog via SOAPaligner. Taxonomic and functional annotations were assigned through alignment against the NR database (for species annotation) and the KEGG pathway database (for functional annotation)[34]. The raw metagenomic sequences are available under NCBI BioProject Accession No. PRJNA1245017.

Functional annotation of non-redundant genes was conducted by BLASTP alignment (e-value < $1e^{-5}$) against the KEGG database. Genes were assigned to KEGG orthologs (KOs) and metabolic pathways based on top BLAST hits. Key functional genes related to carbon, nitrogen, phosphorus, and E3 metabolism were screened using KO identifiers. The abundance of each KO was calculated as the sum of the abundances of all corresponding genes and normalized to transcripts per million (TPM) to facilitate cross-sample

comparison. Taxonomic annotation of ORFs was performed using BLASTP against the NR database (e-value < $1e^{-5}$), with the top hit used for family-level classification. For each key KO, the relative contribution of a taxonomic group was calculated as the proportion of the total KO abundance accounted for by that group. This method identified microbial taxa central to carbon, nitrogen, phosphorus, and estrogen metabolism within the community.

Statistical analysis

All experimental data were collected in triplicate and statistically assessed by one-way ANOVA using SPSS software. Statistical significance thresholds were assigned based on the following criteria: * $p < 0.05$, ** $p < 0.01$, and *** $p < 0.001$. Correlation analysis and first-order kinetic modeling were performed using OriginPro 2025 software.

Results and discussion

Structural disruption and EPS-mediated adaptation of MBGS under E3 stress

The addition of E3 significantly impacted the granular morphology and characteristics of MBGS, especially at concentrations of 1 and 10 mg/L. E3 was found to disrupt the filamentous structure of *Cyanobacteria* within the MBGS, resulting in structural breakage and membrane rupture (Fig. 1). Consequently, the abundance of *Cyanobacteria*, chlorophyll content, and glycogen content in MBGS were significantly reduced (Fig. 2a, b). As *Cyanobacteria* act as a reticular skeleton for the MBGS[25], their structural disruption and decreased abundance negatively affect the settling performance of the system[22]. At E3 concentrations of 1 and 10 mg/L, MBGS exhibited increased granule size, along with higher SVI_5, and lower ZSV (Fig. 2c; Supplementary Fig. S1). In contrast, 0.1 mg/L E3 might promote the growth and settling performance of MBGS, as evidenced by an increased VSS concentration, a lower SVI_5, and a higher ZSV compared to 0 mg/L (Fig. 2c; Supplementary Fig. S1a, S1b).

Additionally, exposure to E3 prompted MBGS to enhance its secretion of EPS (Fig. 2d; Supplementary Fig. S1c), particularly polysaccharides (PS), as a compensatory response to mitigate its toxicity[35]. This response supports two primary protective functions: the formation of a cross-linked physicochemical barrier against xenobiotic intrusion[36]; and the provision of functional groups that facilitate E3 adsorption[37]. FT-IR analysis further confirmed interactions between EPS functional groups and E3 molecules (Fig. 2e; Supplementary Table S2). Key spectral shifts, including N–H, C=O, and COO^- groups from PN, along with O–H, C–O groups from PS, implied they may interact with hydroxyl or ketone groups in E3 and thus serve as the primary adsorption sites for E3. Under high E3 stress (10 mg/L), a marked reduction in proteins (PN) coincided with an increase in the abundance of oxidative stress genes (SOD, CAT; Supplementary Table S3), indicating a metabolic reallocation from polymer synthesis toward essential detoxification processes. The dynamic PN/PS ratio variations further reflect EPS-mediated adaptive strategies. Collectively, these results demonstrate that EPS contributes critically to MBGS resilience through barrier formation and contaminant adsorption, although precise binding mechanisms remain a focus for future investigation.

Inhibition of pollutant removal by MBGS under E3 exposure

As indicated in Fig. 3, high concentrations of E3 (1 and 10 mg/L) significantly inhibited pollutant removal by MBGS, particularly for COD ($p < 0.05$). In contrast, an E3 concentration of 0.1 mg/L enhanced COD removal efficiency, with average COD removal efficiencies increasing

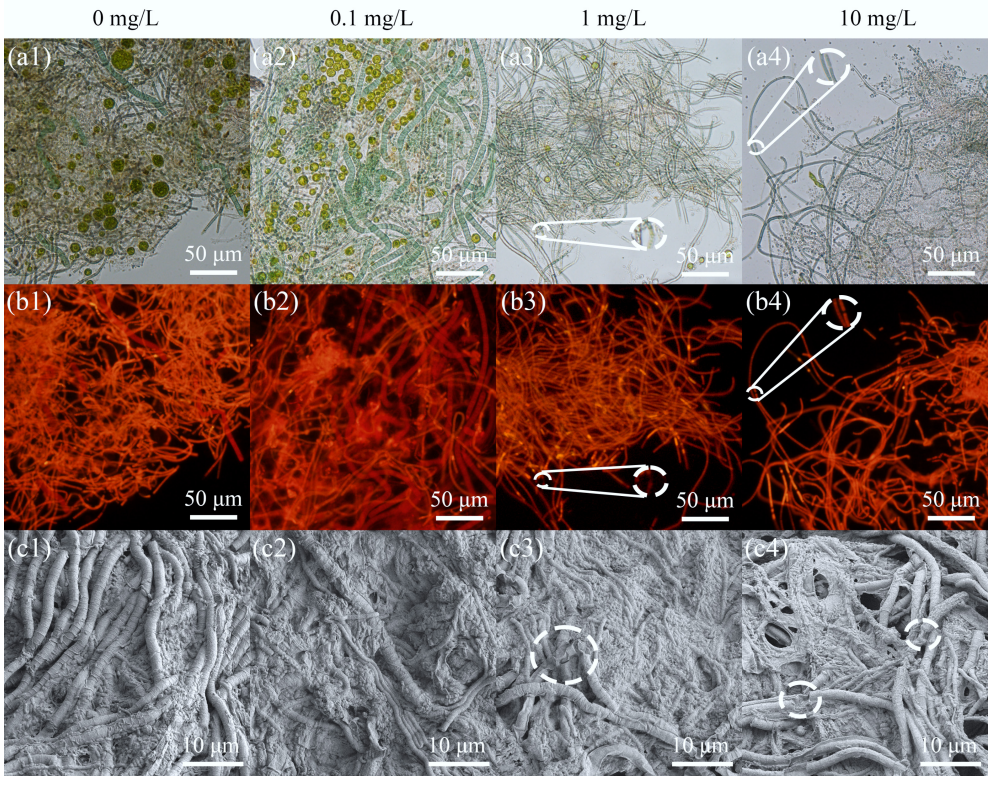

Fig. 1 Microbial morphological characteristics of MBGS under varying estriol (E3) concentrations (0, 0.1, 1, and 10 mg/L). (**a**) White-light, and (**b**) red-light micrographs, with red autofluorescence indicating *Cyanobacteria*. (**c**) SEM images.

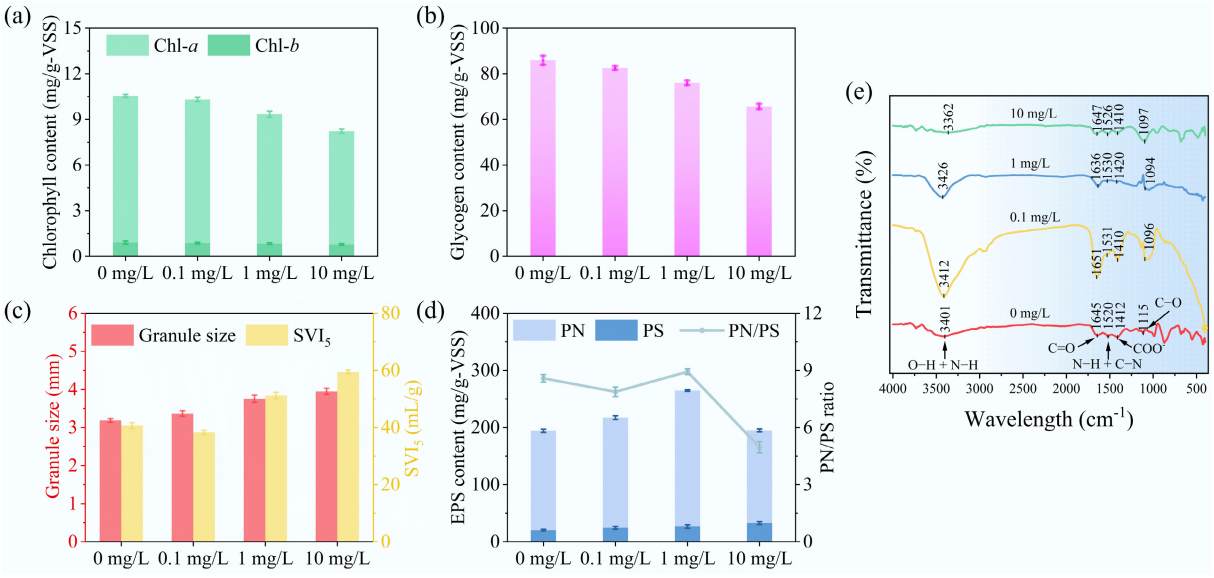

Fig. 2 Physiological and biochemical responses of MBGS to varying estriol (E3) concentrations (0, 0.1, 1, and 10 mg/L). (**a**) Chl-*a* and Chl-*b* contents. (**b**) Glycogen content. (**c**) Granule size and SVI_5. (**d**) EPS content and PN/PS ratio. (**e**) FT-IR spectrum of EPS.

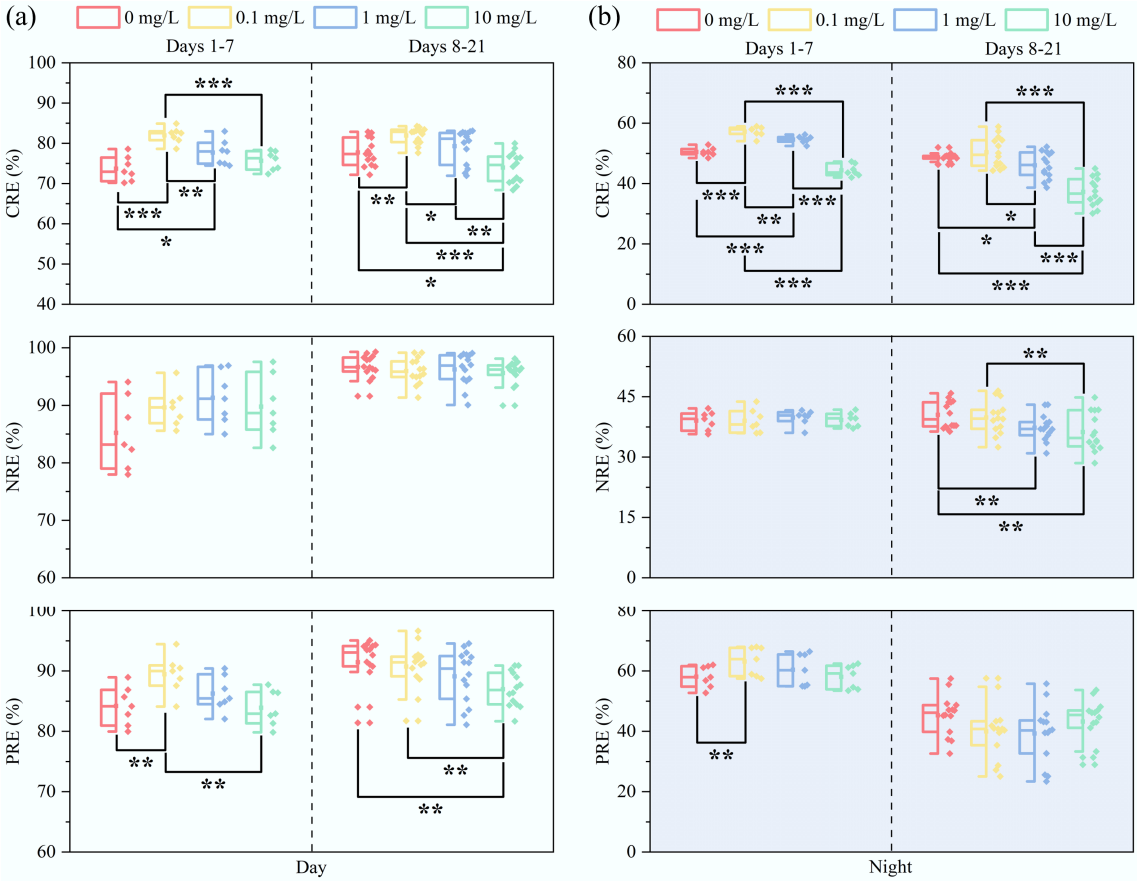

Fig. 3 Diurnal removal performance of pollutant by MBGS under varying estriol (E3) concentrations (0, 0.1, 1, and 10 mg/L). Removal efficiencies (RE) of COD, NH_4^+-N, and PO_4^{3-}-P during (**a**) daytime, and (**b**) nighttime. n = 7 and 14 for days 1–7, and 8–21, respectively. * $p < 0.05$, ** $p < 0.01$, and *** $p < 0.001$.

from 74.4% to 84.1% during the daytime, and from 49.6% to 53.8% at night. During days 8 to 21 of exposure to 10 mg/L E3, nighttime COD removal efficiency experienced a significant decline (Supplementary Fig. S2), likely due to structural damage in *Cyanobacteria* that impaired organic assimilation by MBGS[29]. Although NH_4^+-N and PO_4^{3-}-P removal exhibited similar dependence on cyanobacterial activity (Supplementary Fig. S3a), their underlying mechanisms were distinct. Importantly, NH_4^+-N removal depends on light availability[38], with sufficient daylight irradiation offsetting the reduction in *Cyanobacteria*, causing comparable daytime performance but significant variability

during nighttime. Conversely, PO_4^{3-}-P removal exhibited compromised diurnal variation, as the destruction of *Cyanobacteria* hindered normal nighttime phosphate release[39], ultimately diminishing subsequent phosphorus uptake during the day.

Figure 4 illustrates the cyclical removal performance of pollutants by MBGS under 10 mg/L E3 stress. The removal efficiencies of MBGS for COD, NH_4^+-N, and PO_4^{3-}-P were 70.5%/32.0%, 97.9%/26.1%, and 81.6%/28.4%, respectively, during the daytime and nighttime periods, and they stabilized at 4 h/4 h, 8 h/1 h, and 3 h/1.5 h, respectively. The rapid stabilization and low removal performance of MBGS for NH_4^+-N during nighttime further illustrate the crucial significance of *Cyanobacteria* activity on NH_4^+-N removal[40]. In summary, the MBGS system effectively tolerated and even showed enhanced performance at an E3 concentration of 0.1 mg/L. In contrast, concentrations of 1 and 10 mg/L significantly impaired pollutant removal by disrupting the cellular structures of *Cyanobacteria*.

Removal efficiency and metabolic pathways of E3 by MBGS

Figure 5a, b demonstrates that the MBGS system achieved removal efficiencies of 97.9% during the daytime, and 85.7% during nighttime for 0.1 mg/L E3. In contrast, the removal efficiencies for 1 mg/L E3 were 44.5% and 19.6%, and for 10 mg/L E3, they were 12.6% and 10.6%, respectively. The MBGS system demonstrated significant adaptability when exposed to low concentrations of E3 (0.1 mg/L), showing a progressive enhancement in removal efficiency over time. However, when challenged with higher E3 concentrations (1 and 10 mg/L), the system demonstrated no significant capacity for adaptation, resulting in lower biodegradation performance. Based on kinetic analysis of the time-course removal data at 10 mg/L E3, the first-order degradation rate constant was significantly higher during the day (0.0121 h^{-1}) than during the night (0.0053 h^{-1}) (Fig. 5c, d; Supplementary Fig. S4). The nocturnal decrease in E3 removal efficiency was attributed to oxygen limitation, which suppressed the metabolic activity of heterotrophic degraders, thereby highlighting the crucial role of photosynthetic oxygen production in sustaining biodegradation of E3. Additionally, EPS adsorption accounted for 21.9% of the total E3 removal within 12 h in the live system. The adsorption process was characterized by a rapid initial phase, reaching equilibrium within approximately 1.5 h, followed by a stable phase with no significant further removal, confirming the absence of biodegradation in the inactivated systems (Supplementary Fig. S5). This clearly indicates that adsorption plays a significant, but not dominant, role in the initial phase of E3 removal, facilitating the subsequent biodegradation by immobilizing the substrate on the biomass.

Through UHPLC-HRMS analysis, four estrogenic compounds (E3, E1, A1, and B1) were identified in the effluent samples, as shown in Supplementary Fig. S6. Recent studies indicate that the biodegradation process begins with the oxidation of E3 to E1, followed by conversion to 4-hydroxyestrone (4-OH-E1)[18]. Although this transient intermediate was not detected in the aqueous matrix, several

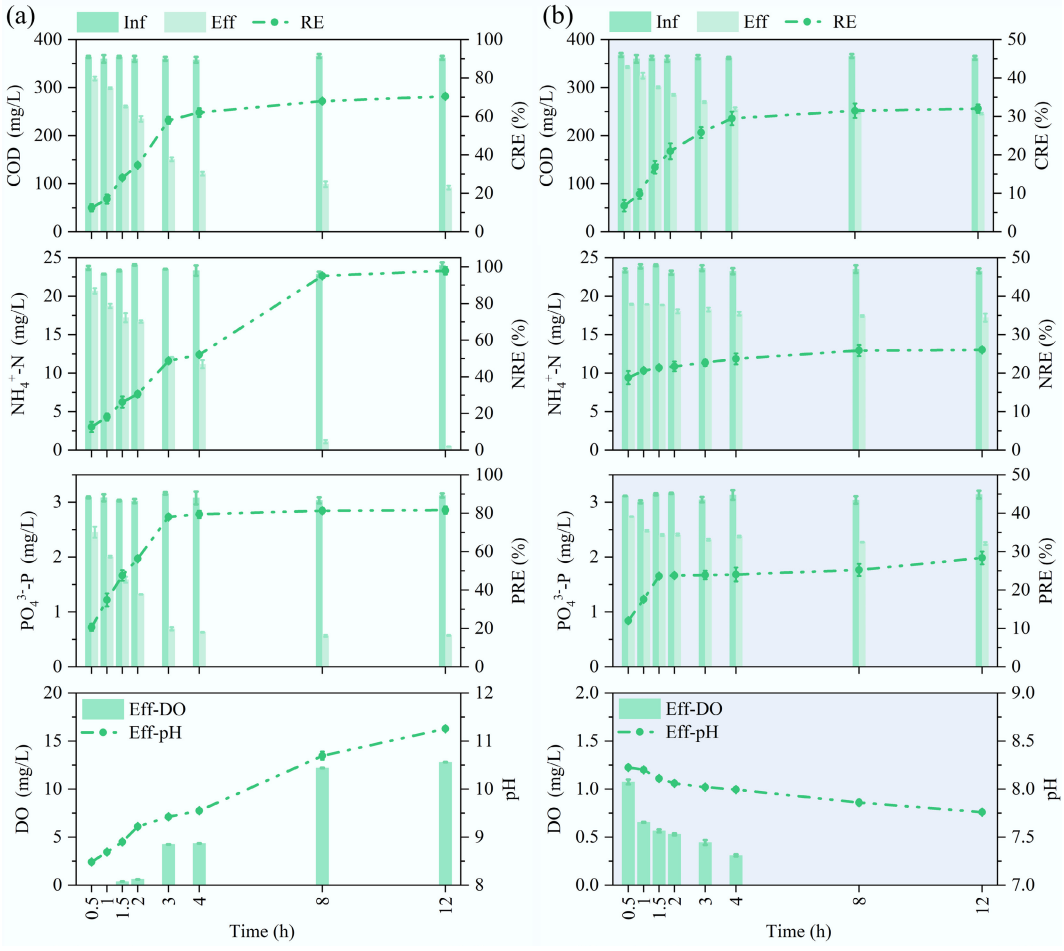

Fig. 4 Batch removal performance of pollutants by MBGS and effluent characteristics at 10 mg/L estriol (E3) addition. Removal efficiencies (RE) of COD, NH_4^+-N, and PO_4^{3-}-P, along with effluent DO concentration and pH value, during (**a**) daytime, and (**b**) nighttime.

studies have clearly demonstrated that it serves as a crucial node in the *Proteobacteria*-mediated degradation pathway of E1[23,41,42]. The absence of 4-OH-E1 may be attributed to its rapid enzymatic conversion[43,44]. Subsequent metabolism diverges through stereospecific oxidation reactions, yielding metabolite A1 via the 4,5-*seco* pathway and metabolite B1 via the 9,10-*seco* pathway (Fig. 5e). Notably, the terminal metabolites A1 and B1 display a markedly lower ecotoxicological risk relative to E3, as evidenced by reduced bioconcentration factors and mutagenicity, suggesting an environmentally safer profile (Supplementary Table S4). Future investigations will employ isotope tracing, quantitative monitoring of intermediates, and advanced molecular techniques to elucidate the degradation pathways and the transformation kinetics of intermediates.

Microbial response mechanisms revealed by metagenomic analysis

Microbial community shift and Cyanobacteria decline under E3 stress

The microbial community was primarily composed of *Cyanobacteria* (33.5%), *Betaproteobacteria* (19.1%), *Gammaproteobacteria* (13.0%), and *Alphaproteobacteria* (11.8%). At the family level, *Oculatellaceae* (12.0%), *Leptolyngbyaceae* (9.5%), *Sphaerotilaceae* (7.2%), and *Rhodanobacteraceae* (6.7%) were dominant in the MBGS (Fig. 6a). The introduction of E3 significantly reduced the relative abundance of *Cyanophyceae* (including *Oculatellaceae*, *Leptolyngbyaceae*) and *Comamonadaceae* from the *Betaproteobacteria* (Fig. 6b, c). In contrast, it stimulated the growth of *Rhodanobacteraceae* and *Xanthomonadaceae* among the *Gammaproteobacteria*, and *Sphingomonadaceae* within the *Alphaproteobacteria* (Fig. 6b, c; Supplemetnary Fig. S3b). Although *Sphingomonadaceae* and *Rhodanobacteraceae* have been reported to degrade E3[18,45], their enrichment did not improve the overall E3 removal efficiency. This outcome likely reflects a functional trade-off resulting from the collapse of *Cyanobacteria*, which compromised both oxygen supply and structural support, counteracting potential degradation gains. The decline in *Leptolyngbyaceae* (key phosphorus-accumulating microalgae[39]) and *Comamonadaceae* (key phosphorus-accumulating bacteria[46]) probably contributed to the diminished PO_4^{3-}-P removal. Notably, *Sphaerotilaceae* reached its peak abundance at an E3 concentration of 0.1 mg/L, coinciding with optimal COD removal. As this family enhances carbon fixation capacity in MBGS[47], its proliferation likely supported improved system function at this concentration.

Correlation analysis indicated significant negative relationships between *Cyanobacteria* and *Gammaproteobacteria*, as well as between *Oculatellaceae* and *Rhodanobacteraceae*/*Xanthomonadaceae* (Fig. 6d, e). This contrasts with previous network analyses that

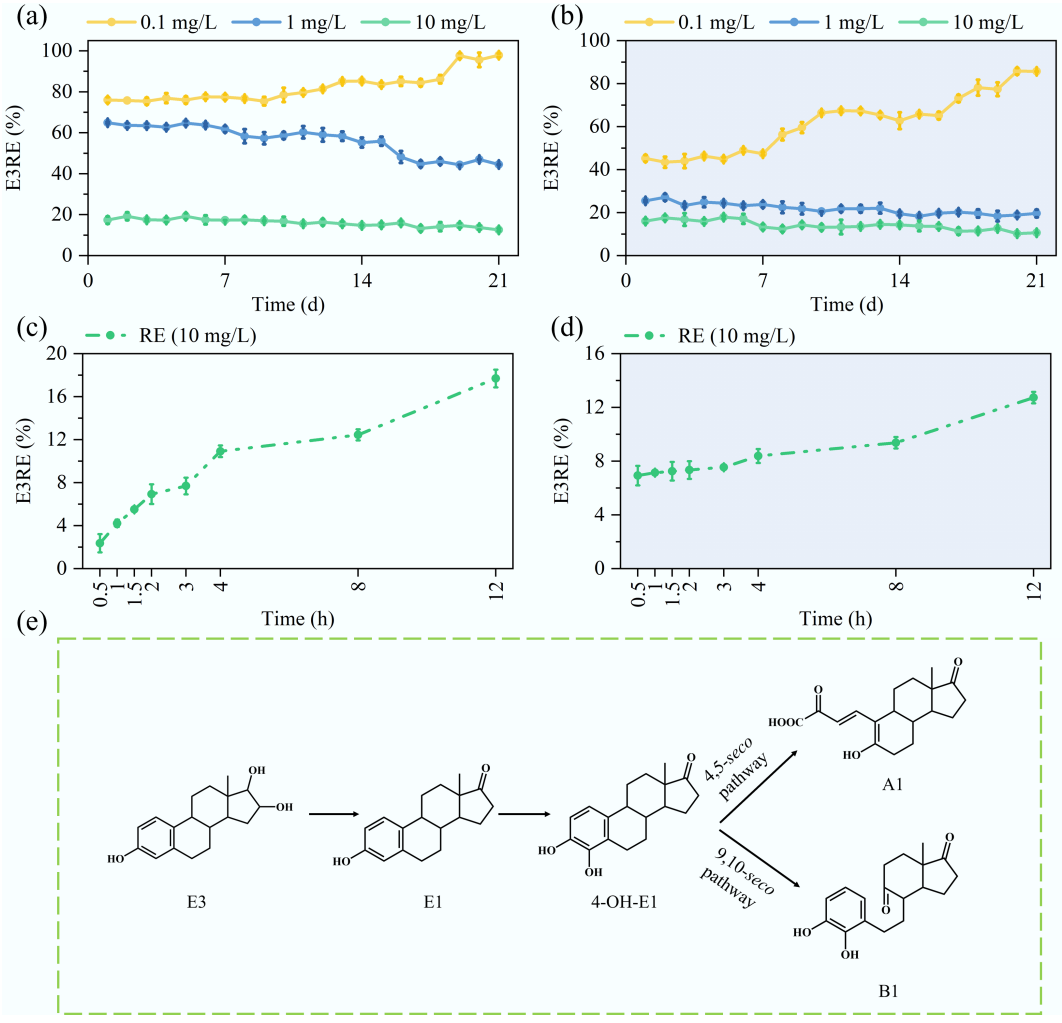

Fig. 5 Diurnal, batch, and metabolic profiling of estriol (E3) removal by MBGS. (**a**), (**b**) Daily removal efficiencies (RE) for 0.1, 1, and 10 mg/L E3, and (**c**), (**d**) batch removal efficiencies (RE) for 10 mg/L E3 during daytime and nighttime. (**e**) Proposed metabolic pathways.

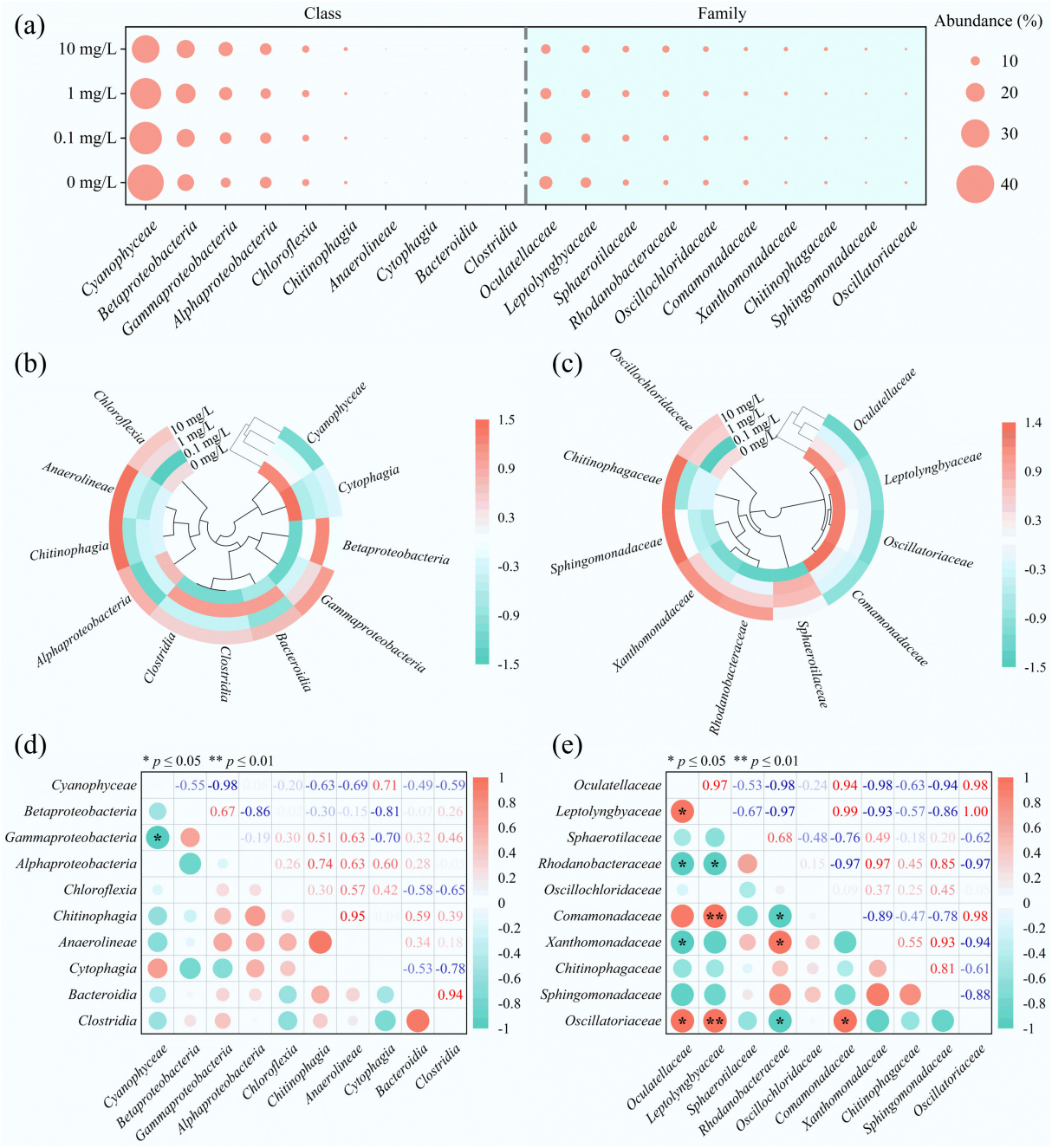

Fig. 6 Microbial community composition of the MBGS under varying estriol (E3) concentrations at class and family levels. (**a**) Relative abundance bubble plot, with circle size indicating abundance. (**b**), (**c**) Clustering heat maps, color intensity reflecting abundance changes. (**d**), (**e**) Correlation plots, with red and green denoting positive and negative correlations, respectively.

identified a strong positive correlation between *Cyanobacteria* and *Gammaproteobacteria*[26]. In MBGS, *Cyanobacteria* are essential structural components that maintain granule stability[25]. Collectively, these findings suggest that functional impairment induced by E3 in MBGS primarily results from structural damage to *Cyanobacteria*, disrupting essential microbial interactions, particularly inverting the relationships between *Oculatellaceae* and *Rhodanobacteraceae*/*Xanthomonadaceae*. As a result, even though the abundance of these degraders increased, it did not lead to improved E3 degradation efficiency. Future research will employ techniques such as metatranscriptomics of key taxa, targeted inhibition of specific groups, or isolation of key organisms in defined co-cultures to establish direct causal mechanisms linking community structure to the *seco*-pathway dynamics.

Functional gene attenuation and metabolic shifts under E3 exposure

As illustrated in Fig. 7a–c, the MBGS system assimilated carbon, nitrogen, and phosphate through glycolysis/gluconeogenesis (ko00010) and the TCA cycle (ko00020), nitrogen metabolism (ko00910), and oxidative phosphorylation (ko00190), respectively. Key functional genes associated with variations in removal efficiency include the *mqo* linked to the TCA cycle, and *fccA* genes involved in electron transport chain, the *GLU* gene associated with nitrogen metabolism, and the *ppk1* and *atpA* genes involved in oxidative phosphorylation (Fig. 7d).

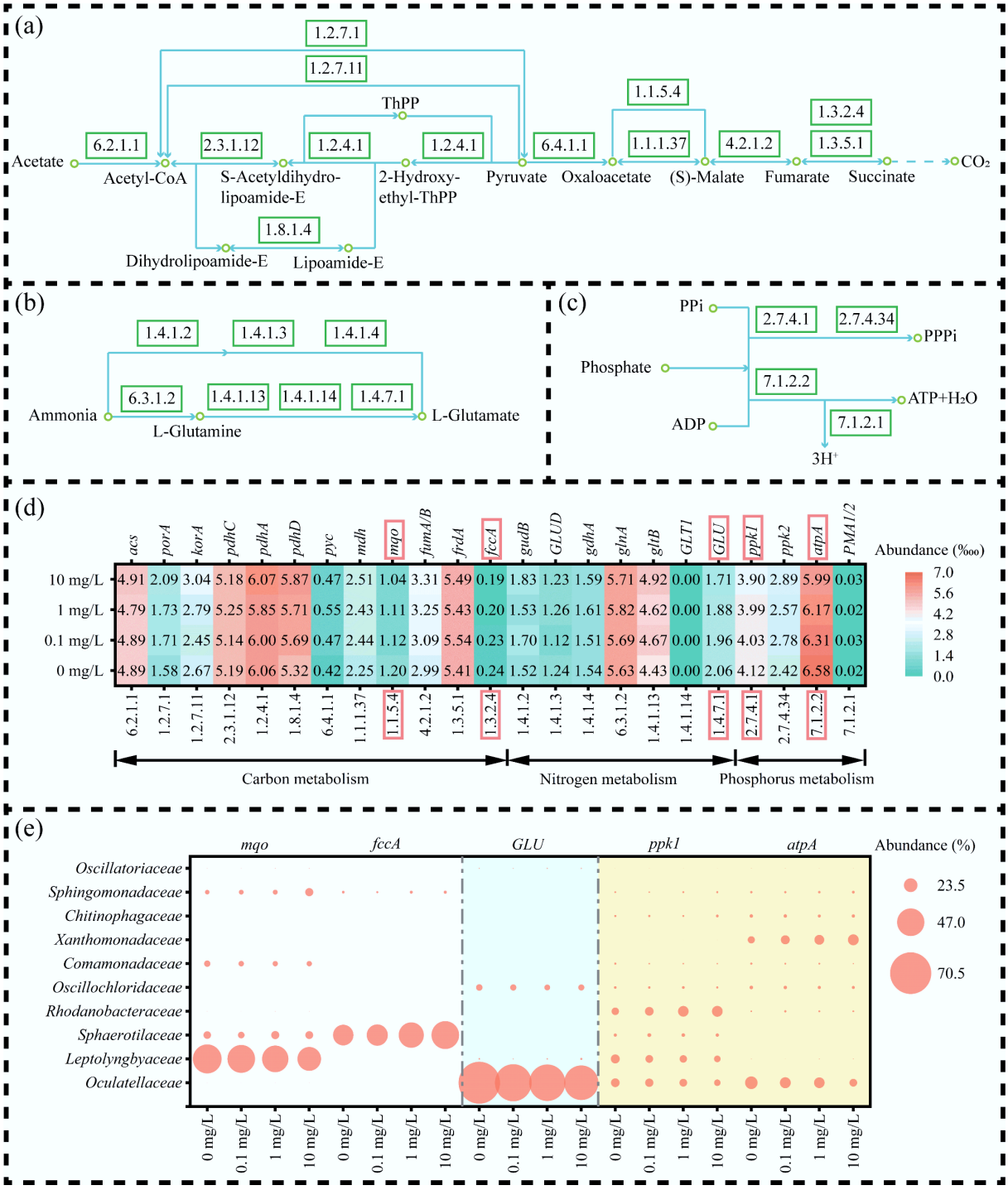

Fig. 7 Functional metabolic response of MBGS to varying estriol (E3) concentrations across carbon, nitrogen, and phosphate pathways. (**a**)–(**c**) Metabolic pathways of carbon, nitrogen, and phosphorus, respectively. (**d**) Relative abundance (‰) of key functional genes, with color intensity indicating abundance level. (**e**) Microbial contribution (%) to functional gene, with circle size indicating contribution.

The observed decline in functional gene abundance was primarily induced by E3 stress, which targeted the core of microbial metabolic pathways. This perturbation severely disrupted energy generation, as evidenced by the reduced abundance of key genes involved in ATP production (e.g., *atpA*, *mqo*, and *fccA*), resulting in a critical shortage of ATP. The ensuing energy crisis directly starved the highly ATP-dependent processes responsible for COD removal and phosphorus uptake. Critically, polyphosphate kinase (*ppk1*)-mediated phosphorus assimilation was severely impeded due to the lack of ATP substrate[48], leading to a failure in biological phosphorus removal. Furthermore, the stress compromised biosynthetic capacity, exemplified by reduced *GLU* gene, which disrupted nitrogen assimilation and thereby *de novo* protein synthesis, aggravating the functional collapse of the treatment system.

Further analysis indicated that increasing E3 concentrations significantly reduced the contributions of the dominant families

Oculatellaceae and *Leptolyngbyaceae* to the *mqo*, *GLU*, *ppk1*, and *atpA* genes (Fig. 7e). *Oculatellaceae* and *Leptolyngbyaceae* primarily regulated the *mqo* and *GLU* genes, influencing the ability of the MBGS system to remove carbon and nitrogen. The reduced involvement of *Leptolyngbyaceae* and *Comamonadaceae* in the *ppk1* and *atpA* genes critically impacted phosphorus removal. The increased contribution of *Sphaerotilaceae* to the *fccA* gene likely explains the optimal COD removal efficiency observed at an E3 concentration of 0.1 mg/L. Furthermore, *Xanthomonadaceae* enhanced the energy metabolism of the MBGS system under E3 stress by increasing their contributions to the *atpA* gene.

The impact of E3 addition on the pollutant removal performance of the MBGS system was concentration-dependent. At high concentrations (1 and 10 mg/L), E3 significantly disrupted the filamentous structure and cellular integrity of *Cyanobacteria*, thereby impairing the structural stability and settling ability of the MBGS. This structural damage resulted in a marked decline in removal efficiencies for COD, NH_4^+-N, and PO_4^{3-}-P, particularly during nighttime. Metagenomic analysis further revealed that E3 altered the microbial community composition by suppressing key functional taxa such as *Oculatellaceae*, *Leptolyngbyaceae*, and *Comamonadaceae*, while promoting the proliferation of *Sphingomonadaceae*, *Rhodanobacteraceae*, and *Xanthomonadaceae*. These shifts disrupted microbial interactions and reduced the abundance of critical functional genes (e.g., *mqo*, *GLU*, *ppk1*, *atpA*). In contrast, the low E3 concentration (0.1 mg/L) slightly enhanced system performance, likely due to the increased abundance of *Sphaerotilaceae* and its contribution to the *fccA* gene, which is involved in carbon metabolism.

Biodegradation mechanism of E3 by MBGS

The microbial transformation of E3 to E1 was primarily catalyzed by 17β-hydroxysteroid dehydrogenase (EC: 1.1.1.51, encoded by *hshA*)[49]. Subsequent aerobic catabolism of the steroidal A-ring involved a series of key reactions, including initial hydroxylation and ring-opening mediated by a two-component system comprising HSA monooxygenase (EC: 1.14.14.12, *hsaA*) and its reductase component (EC: 1.5.1.-, *hsaB*), which generated a catecholic intermediate (4-OH-E1). This intermediate was then cleaved by 4,5-DHSA dioxygenase (EC: 1.13.11.25, *hsaC*), which performed intra-diol fission of the aromatic ring, leading to the production of A1. Alternatively, the classical meta-cleavage pathway was facilitated by catechol 2,3-dioxygenase (EC 1.13.11.2, *xylE*), leading to the formation of B1 (Fig. 8a). Gene abundance analysis demonstrated a concentration-dependent increase in *hshA*, *hsaA*, and *hsaB* under E3 exposure, with *hshA* exhibiting the highest abundance (0.730‰ at 10 mg/L), suggesting its dominant role in the initial transformation step. In contrast, *hsaC* showed relatively low abundance (0.044‰ at 10 mg/L), implying a potential rate-limiting function. The sharp decline in *hsaC* and *xylE* abundance at 10 mg/L E3 may partially account for the suboptimal removal efficiency observed at this concentration (Fig. 8b).

From the perspective of functional microbial contributions, *Sphingomonadaceae* dominated the abundance of *hshA*, *hsaA*, *hsaB*, and *hsaC*, accounting for more than 58% of *hsaC* at 10 mg/L, highlighting their pivotal role in aromatic ring degradation[50]. Meanwhile, *Rhodanobacteraceae* were mainly associated with *hshA* and *hsaB*, underscoring their importance in the initial transformation of the substrate. The superior removal efficiency observed at 0.1 mg/L aligns with the concurrent abundance peak of key functional genes contributed by these two families (Fig. 8c). Overall, the metabolic conversion of E3 into E1, 4-OH-E1, A1, and B1 was mediated by the coordinated activity of enzymes encoded by *hshA*, *hsaA*, *hsaB*, *hsaC*, and *xylE*, with keystone taxa including *Sphingomonadaceae* and *Rhodanobacteraceae* playing critical roles in maintaining pathway efficacy.

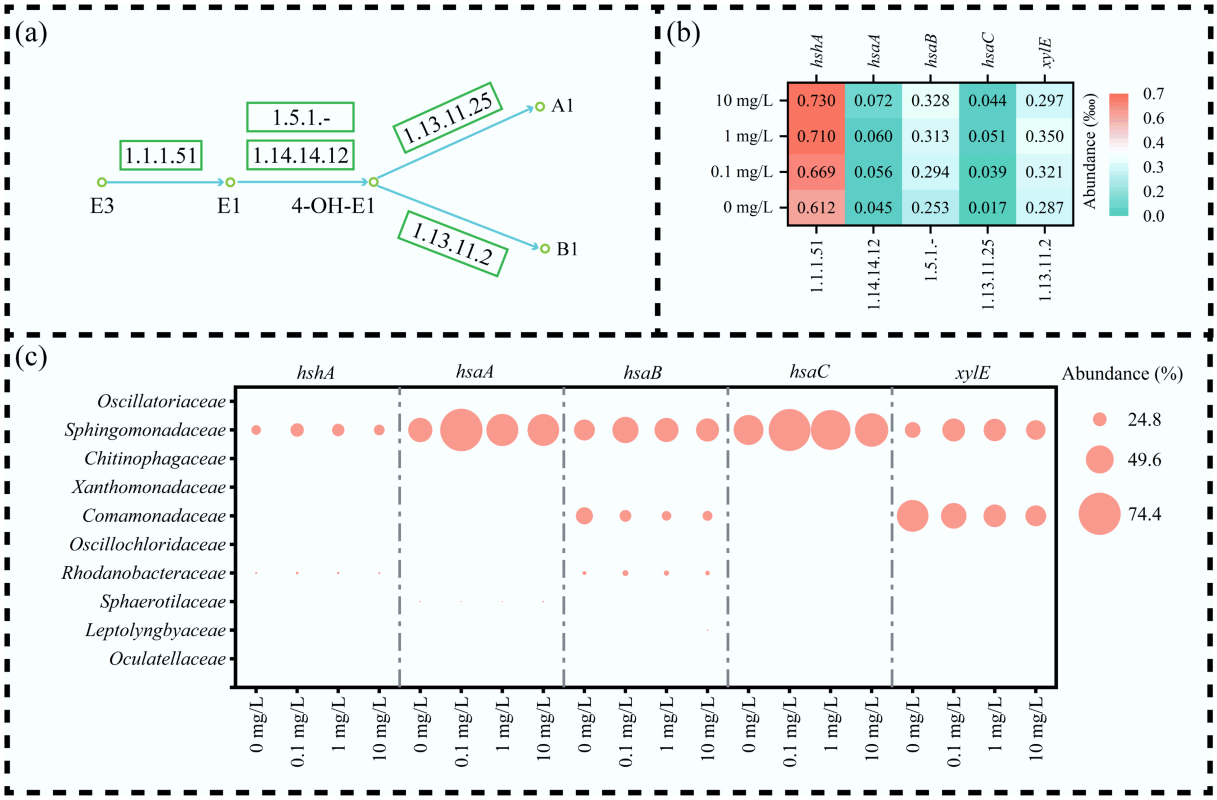

Fig. 8 Functional metabolism of estriol (E3) by MBGS. (**a**) Metabolic pathways and associated enzymes of E3. (**b**) Relative abundance (‰) of key functional genes, with color intensity indicating abundance level. (**c**) Microbial contribution (%) to functional gene, with circle size indicating contribution.

Conclusions

This study elucidates the effects of E3 on the structure, performance, microbial dynamics, and function of MBGS. At a low concentration of 0.1 mg/L, E3 promoted the growth of *Sphaerotilaceae*, which in turn improved COD removal. Conversely, exposure to higher E3 concentrations of 1 and 10 mg/L caused significant damage to *Cyanobacteria*, leading to impaired granular structure and decreased pollutant removal efficiency. The significant inhibition of keystone taxa (*Oculatellaceae*, *Leptolyngbyaceae*, and *Comamonadaceae*) and their associated functional genes (*mqo*, *GLU*, *ppk1*, and *atpA*) was indentified as the primary cause of the decline in removal performance. In response, the MBGS system enhanced the conversion of E3 to putative metabolites A1 and B1 by increasing the abundance of *Sphingomonadaceae* and *Rhodanobacteraceae*, which contributed significantly to key functional genes (*hshA*, *hsaA*, *hsaB*, *hsaC*, and *xylE*) essential for E3 removal. Concurrently, *Xanthomonadaceae* maintained partial energy metabolism functions by elevating their contribution to the *atpA* gene. Collectively, these findings highlight the importance of *Cyanobacteria*-driven structural integrity and functional microbial synergies in maintaining the resilience of the MBGS system against estrogenic stress. This work provides critical insights for developing robust MBGS-based technologies for treating wastewater contaminated with EDCs.

Supplementary information

It accompanies this paper at: https://doi.org/10.48130/biocontam-0025-0004

Author contributions

The authors confirm their contributions to the paper as follows: material preparation, data collection and analysis: Shi Y, Chen C, Ding B, Shu Y, Feng J; writing the first draft of manuscript: Shi Y; commenting on draft manuscript: all authors. All authors reviewed the results and approved the final version of the manuscript.

Data availability

The datasets used or analyzed in the current study are available from the corresponding author upon reasonable request.

Funding

The research leading to these results was funded by the National Natural Science Foundation of China under Grant Agreement Nos 52261135627 and 52270048.

Declarations

Generative AI and AI-assisted technologies

During the preparation of this work, the authors used ChatGPT to improve readability. After using this tool, the authors reviewed and edited the content as needed and take full responsibility for the content of the publication.

Competing interests

The authors declare that there is no conflict of interest.

Author details

[1]Department of Water and Wastewater Engineering, School of Urban Construction, Wuhan University of Science and Technology, Wuhan 430065, China; [2]Hubei Key Laboratory for Efficient Utilization and Agglomeration of Metallurgic Mineral Resources, School of Resource and Environmental Engineering, Wuhan University of Science and Technology, Wuhan 430065, China; [3]Institute of Artificial Intelligence, Huazhong University of Science and Technology, Wuhan 430074, China; [4]Key Laboratory of Water and Sediment Sciences of Ministry of Education, State Key Laboratory of Water Environment Simulation, School of Environment, Beijing Normal University, Beijing 100875, China

References

[1] Xiao Y, Han D, Currell M, Song X, Zhang Y. 2023. Review of Endocrine Disrupting Compounds (EDCs) in China's water environments: implications for environmental fate, transport and health risks. *Water Research* 245:120645

[2] Pei J, Peng J, Wu M, Zhan X, Wang D, et al. 2025. Analyzing the potential targets and mechanisms of chronic kidney disease induced by common synthetic Endocrine Disrupting Compounds (EDCs) in Chinese surface water environment using network toxicology and molecular docking techniques. *Science of The Total Environment* 958:177980

[3] Lerdsuwanrut N, Zamani R, Akrami M. 2025. Environmental and human health risks of estrogenic compounds: a critical review of sustainable management practices. *Sustainability* 17:491

[4] Bilal M, Barceló D, Iqbal HMN. 2021. Occurrence, environmental fate, ecological issues, and redefining of endocrine disruptive estrogens in water resources. *Science of The Total Environment* 800:149635

[5] Ting YF, Praveena SM. 2017. Sources, mechanisms, and fate of steroid estrogens in wastewater treatment plants: a mini review. *Environmental Monitoring and Assessment* 189:178

[6] Tang Z, Liu ZH, Wang H, Dang Z, Yin H, et al. 2020. Trace determination of eleven natural estrogens and insights from their occurrence in a municipal wastewater treatment plant and river water. *Water Research* 182:115976

[7] Kumar AK, Sarma PN, Mohan SRV. 2016. Incidence of selected endocrine disrupting estrogens in water bodies of Hyderabad and its relation to water quality parameters. *Environmental Engineering and Management Journal* 15:315–325

[8] Boro D, Chirania M, Verma AK, Chettri D, Verma AK. 2025. Comprehensive approaches to managing emerging contaminants in wastewater: identification, sources, monitoring and remediation. *Environmental Monitoring and Assessment* 197:456

[9] Bai L, Liu X, Wu Y, Wang C, Wang C, et al. 2024. Ecological determinants of 17α-ethynylestradiol biodegradation: unveiling unique microbial community assemblages in lake sediments under nitrate or sulfate reduction. *Journal of Cleaner Production* 446:141400

[10] Zhang JN, Chen J, Yang L, Zhang M, Yao L, et al. 2021. Occurrence and fate of androgens, progestogens and glucocorticoids in two swine farms with integrated wastewater treatment systems. *Water Research* 192:116836

[11] Sim WJ, Lee JW, Shin SK, Song KB, Oh JE. 2011. Assessment of fates of estrogens in wastewater and sludge from various types of wastewater treatment plants. *Chemosphere* 82:1448–1453

[12] He YJ, Chen W, Zheng XY, Wang XN, Huang X. 2013. Fate and removal of typical pharmaceuticals and personal care products by three different treatment processes. *Science of The Total Environment* 447:248–254

[13] Fredj SB, Nobbs J, Tizaoui C, Monser L. 2015. Removal of estrone (E1), 17β-estradiol (E2), and 17α-ethinylestradiol (EE2) from wastewater by liquid–liquid extraction. *Chemical Engineering Journal* 262:417–426

[14] Lalik A, Szreder J, Grymel M, Żabczyński S, Bajkacz S, et al. 2025. Estrogens and progestogens in environmental waters: analytical chemistry and biosensing perspectives on methods, challenges, and trends. *Analytical Chemistry* 97:8654–8683

[15] Latosińska J, Grdulska A. 2025. A review of methods for the removal of endocrine-disrupting compounds with a focus on oestrogens and pharmaceuticals found in wastewater. *Applied Sciences* 15:6514

[16] Yang J, Li H, Ran Y, Chan K. 2014. Distribution and bioconcentration of endocrine disrupting chemicals in surface water and fish bile of the Pearl River Delta, South China. *Chemosphere* 107:439–446
[17] Zhang Z, Feng Y, Liu Y, Sun Q, Gao P, et al. 2010. Kinetic degradation model and estrogenicity changes of EE2 (17α-ethinylestradiol) in aqueous solution by UV and UV/H_2O_2 technology. *Journal of Hazardous Materials* 181:1127–1133
[18] Liu X, Wang Z, Wang X, Liu J, Waigi MG. 2024. Conversion of estriol to estrone: a bacterial strategy for the catabolism of estriol. *Ecotoxicology and Environmental Safety* 280:116564
[19] Abouhend AS, McNair A, Kuo-Dahab WC, Watt C, Butler CS, et al. 2018. The oxygenic photogranule process for aeration-free wastewater treatment. *Environmental Science & Technology* 52:3503–3511
[20] Ji B, Zhang M, Gu J, Ma Y, Liu Y. 2020. A self-sustaining synergetic microalgal-bacterial granular sludge process towards energy-efficient and environmentally sustainable municipal wastewater treatment. *Water Research* 179:115884
[21] Sun XL, Wang Y, Xiong HQ, Wang ST, Fang YC, et al. 2023. Removal of environmental estrogens from wastewater by microalgae under the influence of bacteria. *Journal of Cleaner Production* 414:137635
[22] Chen B, Liang H, Li A, Ji B, Zhang X, et al. 2025. Impact of ibuprofen on microalgal-bacterial granular sludge: metabolic pathways, functional gene responses and biodegradation mechanisms. *Journal of Hazardous Materials* 492:138180
[23] Chen YL, Yu CP, Lee TH, Goh KS, Chu KH, et al. 2017. Biochemical mechanisms and catabolic enzymes involved in bacterial estrogen degradation pathways. *Cell Chemical Biology* 24:712–724.e7
[24] Zhao K, Si T, Liu S, Liu G, Li D, et al. 2024. Co-metabolism of microorganisms: a study revealing the mechanism of antibiotic removal, progress of biodegradation transformation pathways. *Science of The Total Environment* 954:176561
[25] Kong L, Feng Y, Du W, Zheng R, Sun J, et al. 2023. Cross-feeding between filamentous *Cyanobacteria* and symbiotic bacteria favors rapid photogranulation. *Environmental Science & Technology* 57:16953–16963
[26] Shi Y, Ji B, Li A, Zhang X, Liu Y. 2024. Enhancing the performance of microalgal-bacterial systems with sodium bicarbonate: a step forward to carbon neutrality of municipal wastewater treatment. *Water Research* 266:122345
[27] Li SN, Zhang C, Li F, Ren NQ, Ho SH. 2023. Recent advances of algae-bacteria consortia in aquatic remediation. *Critical Reviews in Environmental Science and Technology* 53:315–339
[28] Ren Z, Li H, Sun P, Fu R, Bai Z, et al. 2024. Development and challenges of emerging biological technologies for algal-bacterial symbiosis systems: a review. *Bioresource Technology* 413:131459
[29] Shi Y, Xu C, Xu K, Chen C, Li A, et al. 2025. Metabolic responses of microalgal-bacterial granular sludge to enrofloxacin and sulfamethoxazole exposure. *Bioresource Technology* 429:132516
[30] APHA. 2005. *Standard methods for the examination of water and wastewater*. American Public Health Association, Washington, DC, USA
[31] Wang C, Xu C, Chen F, Tang X. 2011. Simultaneous determination of three naturally occurring estrogens in environmental waters by high-performance liquid chromatography. *Journal of Separation Science* 34:2371–2375
[32] EPA. 2022. *Toxicity Estimation Software Tool (TEST) The United States Environmental Protection Agency's Center for Computational Toxicology and Exposure*. Durham, NC, USA
[33] Huang W, Gong B, Wang Y, Lin Z, He L, et al. 2020. Metagenomic analysis reveals enhanced nutrients removal from low C/N municipal wastewater in a pilot-scale modified AAO system coupling electrolysis. *Water Research* 173:115530
[34] Shi Y, Xu C, Ji B, Li A, Zhang X, et al. 2024. Microalgal-bacterial granular sludge can remove complex organics from municipal wastewater with algae-bacteria interactions. *Communications Earth & Environment* 5:347
[35] Zhang Y, Hong Y, Wang X. 2023. Recent advances on using functional materials to increase the pollutant removal capabilities of microalgae and bacteria: especially for their symbiotic systems. *Current Pollution Reports* 9:272–291
[36] Flemming HC, Neu TR, Wingender J. 2016. *The perfect slime: microbial extracellular polymeric substances (EPS)*. Volume 15. London, UK: IWA Publishing doi: 10.2166/9781780407425
[37] Gao JF, Zhang Q, Wang JH, Wu XL, Wang SY, et al. 2011. Contributions of functional groups and extracellular polymeric substances on the biosorption of dyes by aerobic granules. *Bioresource Technology* 102:805–813
[38] Wang S, Zhang Y, Ge H, Hou H, Zhang H, et al. 2023. Cultivation of algal-bacterial granular sludge and degradation characteristics of tetracycline. *Water Environment Research* 95:e10846
[39] Ji B, Zhang M, Wang L, Wang S, Liu Y. 2020. Removal mechanisms of phosphorus in non-aerated microalgal-bacterial granular sludge process. *Bioresource Technology* 312:123531
[40] Jia H, Yuan Q. 2018. Ammonium removal using algae-bacteria consortia: the effect of ammonium concentration, algae biomass, and light. *Biodegradation* 29:105–115
[41] Yu CP, Roh H, Chu KH. 2007. 17β-estradiol-degrading bacteria isolated from activated sludge. *Environmental Science & Technology* 41:486–492
[42] Kurisu F, Ogura M, Saitoh S, Yamazoe A, Yagi O. 2010. Degradation of natural estrogen and identification of the metabolites produced by soil isolates of *Rhodococcus* sp. and *Sphingomonas* sp. *Journal of Bioscience and Bioengineering* 109:576–582
[43] Qiu Q, Wang P, Kang H, Wang Y, Tian K, et al. 2019. Genomic analysis of a new estrogen-degrading bacterial strain, *Acinetobacter* sp. DSSKY-A-001. *International Journal of Genomics* 2019:2804134
[44] Bukato K, Kostrzewa T, Gammazza AM, Gorska-Ponikowska M, Sawicki S. 2024. Endogenous estrogen metabolites as oxidative stress mediators and endometrial cancer biomarkers. *Cell Communication and Signaling* 22:205
[45] Wang C, Li J, Zhao B, Wang Y, Liu G. 2014. Isolation and characteristics of 17β-estradiol-degrading *Dyella* spp. strains from activated sludge. *Nature Environment and Pollution Technology* 13:437–440
[46] Qin H, Ji B, Zhang S, Kong Z. 2018. Study on the bacterial and archaeal community structure and diversity of activated sludge from three wastewater treatment plants. *Marine Pollution Bulletin* 135:801–807
[47] Liao X, Chen C, Chang CH, Wang Z, Zhang X, et al. 2012. Heterogeneity of microbial community structures inside the up-flow biological activated carbon (BAC) filters for the treatment of drinking water. *Biotechnology and Bioprocess Engineering* 17:881–886
[48] Sato N, Endo M, Nishi H, Fujiwara S, Tsuzuki M. 2024. Polyphosphate-kinase-1 dependent polyphosphate hyperaccumulation for acclimation to nutrient loss in the cyanobacterium, *Synechocystis* sp. PCC 6803. *Frontiers in Plant Science* 15:1441626
[49] Pratush A, Yang Q, Peng T, Huang T, Hu Z. 2020. Identification of non-accumulating intermediate compounds during estrone (E1) metabolism by a newly isolated microbial strain BH2-1 from mangrove sediments of the South China Sea. *Environmental Science and Pollution Research* 27:5097–5107
[50] Fokina V, Lobastova T, Tarlachkov S, Shutov A, Kazantsev A, et al. 2025. Degradation of C_{19}-steroids and effect of androstenedione on gene expression in *Nocardioides simplex*. *Current Microbiology* 82:143